Journal of Korean Powder Metallurgy Institute
Vol. 8, No. 3, 2001

Processing of Nano-Sized Metal Alloy Dispersed Al_2O_3 Nanocomposites

Sung-Tag Oh, Seok Namkung, Jai-Sung Lee, Hyoung Seop Kim* and Tohru Sekino**
Department of Metallurgy and Materials Science, Hanyang University, Ansan 425-791, Korea
**Department of Metallurgical Engineering, Chungnam National University, Taejon 305-764, Korea*
***Institute of Scientific and Industrial Research, Osaka University, Osaka 567-0047, Japan*
(Received July 12, 2001)

Abstract An optimum route to fabricate the ferrous alloy dispersed Al_2O_3 nanocomposites such as Al_2O_3/Fe-Ni and Al_2O_3/Fe-Co with sound microstructure and desired properties was investigated. The composites were fabricated by the sintering of powder mixtures of Al_2O_3 and nano-sized ferrous alloy, in which the alloy was prepared by solution-chemistry routes using metal nitrates powders and a subsequent hydrogen reduction process. Microstructural observation of reduced powder mixture revealed that the Fe-Ni or Fe-Co alloy particles of about 20 nm in size homogeneously surrounded Al_2O_3, forming nanocomposite powder. The sintered Al_2O_3/Fe-Ni composite showed the formation of $FeAl_2O_4$ phase, while the reaction phases were not observed in Al_2O_3/Fe-Co composite. Hot-pressed Al_2O_3/Fe-Ni composite showed improved mechanical properties and magnetic response. The properties are discussed in terms of microstructural characteristics such as the distribution and size of alloy particles.

Keywords : Nanocomposites, Dispersion of ferrous alloy, Microstructure, Fracture toughness, Magnetic property

1. Introduction

In recent years Niihara and his co-workers[1-3] developed a novel structure so called ceramic nanocomposites, where nano-sized particles were dispersed into ceramic-matrix grains and/or grain boundaries. The mechanical properties were markedly improved by this approach in various nanocomposites systems. For instance, homogeneous dispersion of 5 vol% SiC nanoparticles could increase the strength of hot-pressed Al_2O_3 from 350 MPa to over 1 GPa. In addition to this high strength, the toughness of the Al_2O_3 was improved from 3.25 to 4.7 $MPa \cdot m^{1/2}$ with the SiC additions. Moreover, ceramic nanocomposites with nano-sized functional metals as the dispersion, such as Al_2O_3/Ni[4] or Al_2O_3/Ni-Co[5] have been found to exhibit attractive magnetic functions without loosing their excellent mechanical properties due to the peculiar role of incorporated metal nanoparticles in physical properties.

The success of functional metal dispersed ceramic nanocomposites implies the possibility to introduce new functions into structural ceramics without degradation of the mechanical properties. However, the dispersion phases in the developed ceramic/metal nanocomposites were restricted to the metal with high melting point and the nonferrous alloys. In this study, therefore, the control of microstructure is emphasized to fabricate Al_2O_3/Fe-Ni and Al_2O_3/Fe-Co alloy nanocomposites with enhanced mechanical properties and ferromagnetism. The homogeneous nanocomposite powders are synthesized via solution-chemistry route using Al_2O_3 and metal nitrate powders. Microstructural characteristics and properties of the powders and sintered composites will be discussed.

2. Experimental Procedure

High-purity Fe- and Ni-nitrate ($Fe(NO_3)_3 \cdot 9H_2O$ and $Ni(NO_3)_2 \cdot 6H_2O$, High Purity Chemetals Lab., Japan) were used as source materials for the Fe-50 wt% Ni alloy. Weighed nitrate powders, corresponding to 10 wt% of alloy in the final composite, were initially dissolved in alcohol. Subsequently, α-Al_2O_3 powder (0.2 μm, AKP-53, Sumitomo Chem. Co., Japan) was mixed with the above-mentioned solution and ball milled for 24 h with high purity Al_2O_3 balls. This procedure was also used for synthesis of Al_2O_3/10 wt% Fe-Co alloy powder mixture, in which $Fe(NO_3)_3 \cdot 9H_2O$ and $Co(NO_3)_2 \cdot 6H_2O$ (High Purity Chemetals Lab., Japan) were used as source materials for the Fe-50 wt% Co alloy. Dried mixtures for Al_2O_3 with Fe-Ni and Fe-

Co nitrates were calcined at 400°C and 350°C for 2 h in air, respectively. Then, soft agglomerates of the calcined powders were again wet and dry ball milled for 24 h using Al_2O_3 balls.

The calcined mixture of Al_2O_3/Fe-Ni powder was kept in a graphite die and reduced by using H_2 gas at 700°C for 1 h. Sintering was performed at 1450°C for 1 h in an argon atmosphere with an applied pressure of 30 MPa. In case of Al_2O_3/Fe-Co system, the powder mixtures were uniaxially pressed at a pressure of 44 MPa and subsequently followed by cold isostatic pressing (CIP) at 125 MPa. After CIPing, the compacts were sintered at 1450°C for 2 h in H_2 gas. Sintered specimens were polished using diamond pastes to final lap of 0.5 μm.

Reduction behavior of the calcined powder in hydrogen atmosphere was analyzed by using a thermogravimetry (TG) to monitor the progress of reduction reaction. The phase composition of the powder mixtures and sintered composites was examined via X-ray diffractometry (XRD), using Cu$K\alpha$ radiation. The microstructure was observed using scanning electron microscopy (SEM) and transmission electron microscopy (TEM). The density of the sintered sample was measured using Archimedes principle in toluene. The fracture toughness was measured by indentation fracture (IF) method with Vickers hardness tester (98 N-load applied for 15 s). The magnetization of the specimens was estimated using a vibrating sample magnetometer (VSM) with an applied magnetic field up to ±10 kOe at room temperature.

3. Results and Discussion

3.1. Synthesis and microstructure of nanocomposite powders

The XRD profiles for the starting mixture of Al_2O_3/Fe-Ni system at different processing conditions are shown in Fig. 1. The XRD pattern before calcination (pattern (a) in Fig. 1) contains the characteristic peaks for α-Al_2O_3 and a mixture of Fe- and Ni-nitrate phases. After calcination at 400°C, the metal-nitrates peaks are not observed any more, whereas the lines for α-Al_2O_3, Fe-oxide and NiO are found (pattern (b)). In case of Al_2O_3/Fe-Co system, the XRD analysis revealed that the calcined mixture was composed of α-Al_2O_3, Fe- and Co-oxides.

Figure 2 shows the dimensionless weight changes from a TG experiment for the H_2 reduction process of the calcined Al_2O_3/Fe-Ni and Fe-Co mixtures during heat-up to 700°C with a heating rate of 10°C/min, in

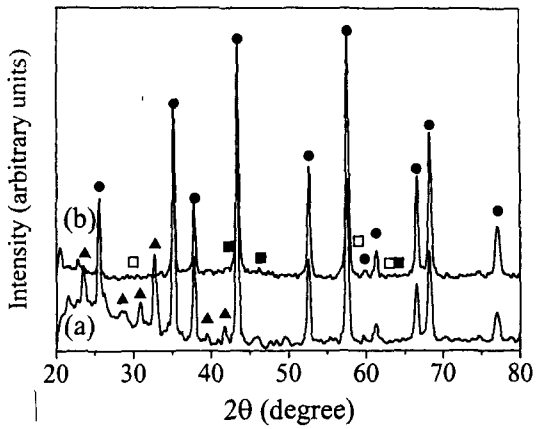

Fig. 1. XRD profiles of the powder mixtures at different stages of processing; (a) initial powder and (b) after calcination in air at 400°C for 2 h ((●) Al_2O_3, (□) Fe-oxide, (■) NiO and (▲) Fe-/Ni-nitrate).

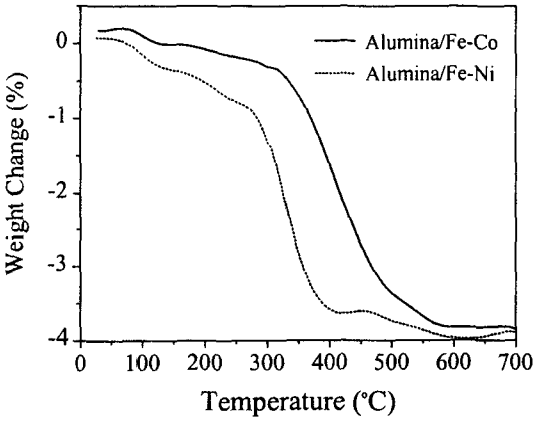

Fig. 2. The dimensionless mass changes for H_2 reduction of the Al_2O_3/Fe-Ni and Fe-Co mixtures, obtained at a scanning rate of 10°C/min.

which the dimensionless weight change (ΔW) represents the ratio of the weight difference to the initial weight. The dimensionless weight changes gradually decrease with increasing temperature and then fall abruptly at 290°C in Al_2O_3/Fe-Ni system and 350°C in Al_2O_3/Fe-Co, and finally the curve reaches the constant value at temperature of above 600°C. Considering the reported reduction behavior of metal oxides,[6,7] it is suggested that the sudden weight changes were due to the formation of water vapor by reduction of Fe-Ni and Fe-Co oxides.

To characterize the microstructure of the reduced powder mixture, the XRD and TEM analyses were

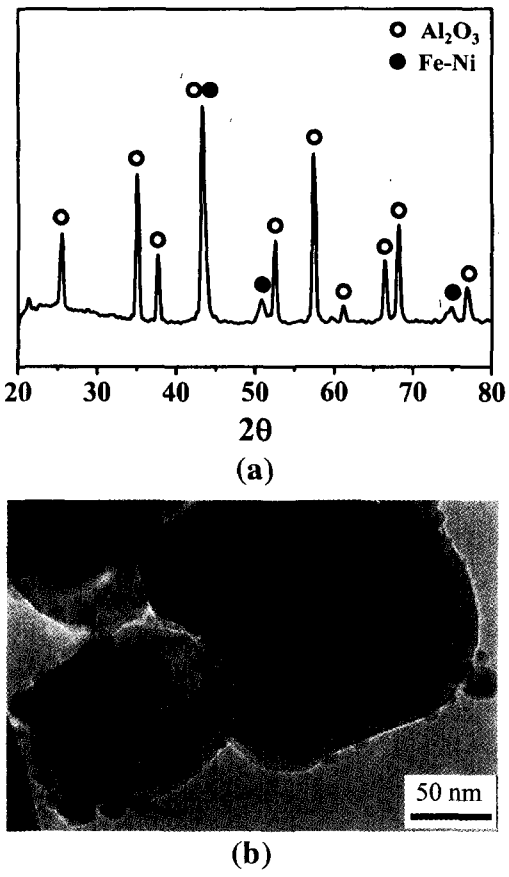

Fig. 3. XRD pattern (a) and TEM micrograph (b) of the Al_2O_3/Fe-Ni mixture reduced at 700°C in H_2 atmosphere. Arrows in Fig. (b) indicate Fe-Ni alloy particles.

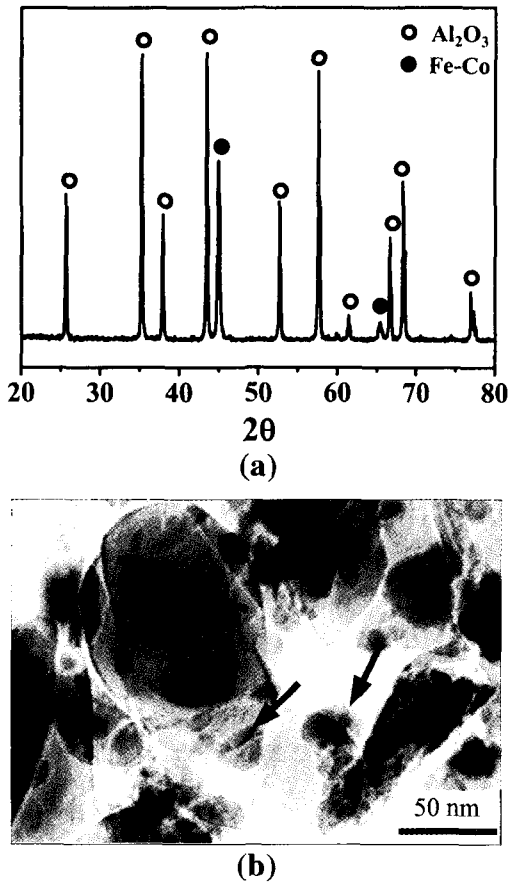

Fig. 4. XRD pattern (a) and TEM micrograph (b) of the Al_2O_3/Fe-Co mixture reduced at 700°C in H_2 atmosphere. Arrows in Fig. (b) indicate Fe-Co alloy particles.

carried out. Fig. 3(a) shows the XRD pattern of the powder mixture reduced at 700°C in hydrogen atmosphere. As shown in the figure, in the region of XRD-resolution, the powder mixture was composed entirely of Al_2O_3 and γ Fe-Ni. Neither residual metal oxides nor a reaction phase was observed. Typical TEM image of the Al_2O_3/10 wt% Fe-Ni composite powder after hydrogen treatment at 700°C is shown in Fig. 3(b). It is clearly shown that the γ Fe-Ni alloy particles of about 20 nm in size were located on Al_2O_3 powders, forming coated nanocomposite powders. It is also revealed from the XRD and TEM analysis for the reduced powder mixture of Al_2O_3/10 wt% Fe-Co that the nano-sized Fe-Co alloy particles were homogeneously dispersed in Al_2O_3 powder surfaces, as shown in Fig. 4(a) and (b).

In the results of microstructure analysis, it is interesting to note that the reduced metal phases were not elemental metals but alloy phases. It means that the complete reduction and alloying of metal oxides to nano-sized alloys in the powder mixture were accomplished by hydrogen reduction process. Recently, Lee et al[6,8] have reported that in-situ alloying process occurs in Fe-Ni system during synthesis of nano-sized Fe-Ni powder by hydrogen reduction of ball milled NiO-Fe_2O_3 powder. Such rapid alloying process, which yielded the stable alloy particles of 20-70 nm in size, was presumed to be possible by the nano-size effect (chemical homogeneity with large surface area) during the reduction process.[9] From consideration of the particle size of alloy phases shown in Fig. 3(b) and 4(b), therefore, the formation of alloy phases in the powder mixture could be explained by in-situ alloying process due to nano-size effect. These results indicate that Al_2O_3 based nanocomposite powder with nano-sized Fe-Ni and Fe-Co alloy particles could be

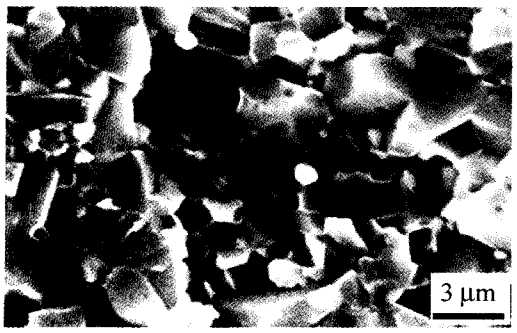

Fig. 5. Fracture surface of the hot-pressed Al_2O_3/10 wt% Fe-Ni composite observed in SEM.

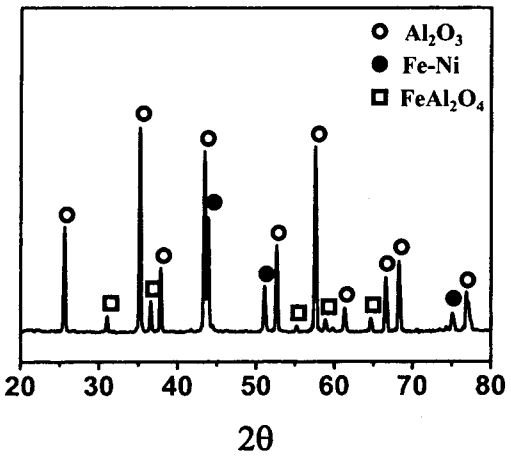

Fig. 6. XRD pattern of the hot-pressed Al_2O_3/10 wt% Fe-Ni composite.

successfully synthesized by these processes.

3.2. Microstructure and properties of hot-pressed Al_2O_3/Fe-Ni composite

Figure 5 shows typical fracture surface for the hot-pressed Al_2O_3/10 wt% Fe-Ni composite. The Ni-Fe alloy particles (the light and spherical phases) are located mainly at the matrix grain boundaries and triple points in the form of finely divided and uniformly distributed particles. However, the Ni-Fe alloy particles showed relatively large size as about 600 nm. Also, XRD analysis indicated that the constituents of hot-pressed composite were found to be Al_2O_3, γ Fe-Ni alloy and $FeAl_2O_4$ as a byproduct, as shown in Fig. 6.

The density and fracture toughness of the composite are summarized in Table 1 and compared to those of monolithic Al_2O_3 prepared under the same conditions. The relative density of specimens was both above 99%.

Table 1. Relative density and fracture toughness for hot-pressed Al_2O_3 and Al_2O_3/10 wt% Fe-Ni composite

Sample	Relative Density (%)	Fracture Toughness (MPa$\sqrt{m}$)
Al_2O_3	99.4	3.3±0.2
Composite	99.4	3.9±0.2

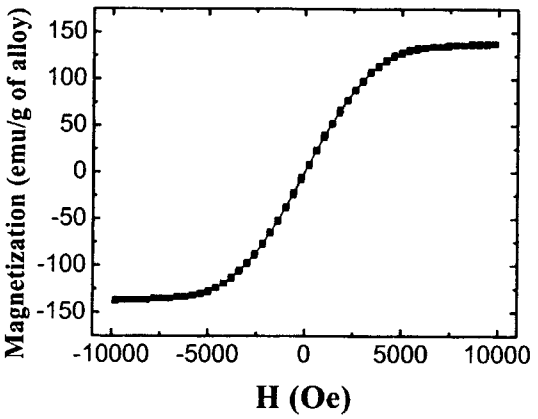

Fig. 7. Room-temperature magnetization versus applied magnetic-field curve for the hot-pressed composite.

The fracture toughness of the composite exhibited an increased value of 3.9±0.2 MPa$\sqrt{m}$, which was 1.2 times larger than that of the monolithic Al_2O_3. SEM observation of the crack propagation revealed the presence of crack deflection and crack bridging,[10] which are thought to be the main reason for the toughness enhancement in this composite system.

Figure 7 shows the magnetization curve of the Al_2O_3/10 wt% Ni-Fe alloy composite. The shape of the magnetization curve and the small hysteresis is typical of ferromagnetic behavior. As the external field was about 10 kOe, magnetization became complete saturation. The measured saturation magnetization, which mentioned the magnetization value obtained at 10 kOe, was 138 emu/g of alloy. The coercive force of the composite showed a value of 16.82 Oe. This experimental result was compared with literature values for pure γ Ni-Fe alloy,[11,12] in which the saturation magnetization and coercive force were 140-180 emu/g and several to some hundred Oe depending on the grain size, respectively.

3.3. Microstructure of sintered Al_2O_3/Fe-Co composite

Typical fracture surface of the Al_2O_3/10 wt% Fe-Co

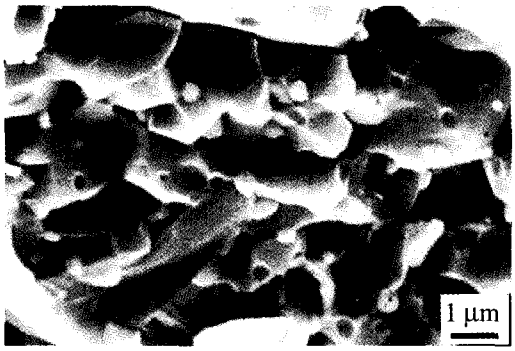

Fig. 8. Fracture surface of the pressureless-sintered Al_2O_3/10 wt% Fe-Co composite observed in SEM.

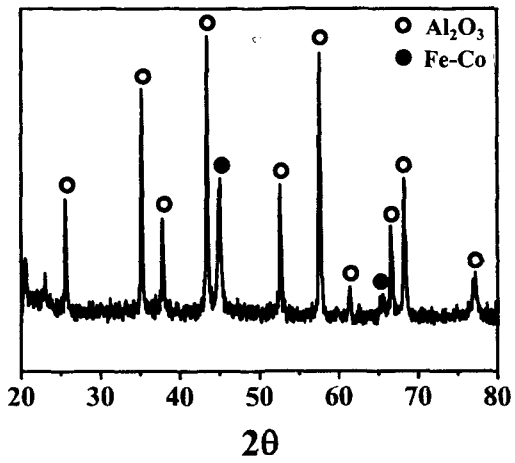

Fig. 9. XRD pattern of the pressureless-sintered Al_2O_3/10 wt% Fe-Co composite.

composite fabricated by pressureless sintering at a temperature of 1450°C for 2 h in H_2 gas is shown in Fig. 8. The Fe-Co alloy particles with an average size of 500 nm are homogeneously located at the matrix grain boundaries and triple points. Fig. 9 shows the XRD pattern of the sintered composite. As shown in the figure, in the region of XRD-resolution, the composite was composed entirely of Al_2O_3 and Fe-Co alloy. It is interesting to note that the reaction phases are not observed in this composite, while the Al_2O_3/Fe-Ni composite shows the formation of $FeAl_2O_4$ phase as shown in Fig. 6. This result indicates that the formation of reaction phase was affected by the alloy system, and thus the ferrous alloy dispersed Al_2O_3 nanocomposites with desired microstructure can be fabricated by using dispersion system of Fe-Co. In this viewpoint, further study for the bulk thermochemistry, especially for the formation of $FeAl_2O_4$ phase and its effect on the mechanical and magnetic properties is currently in progress.

4. Summary

Ferrous alloy dispersed Al_2O_3 nanocomposite powders were successfully synthesized by solution-chemistry routes using powder mixture of Al_2O_3 and metal nitrates. Microstructural observation revealed that ferrous alloy particles with average size of 20 nm were formed by in-situ alloying process and homogeneously distributed in the Al_2O_3 powders. The component of hot-pressed Al_2O_3/10 wt% Fe-Ni composite was found to contain Al_2O_3, γ Fe-Ni alloy and $FeAl_2O_4$ as a byproduct. The composite showed enhanced fracture toughness of 3.9 MPa$\sqrt{m}$ and typical behavior of ferromagnetism with the hysteresis, due to the dispersion of Fe-Ni alloy particles. The Al_2O_3/10 wt% Fe-Co composite was fabricated by pressureless sintering at a temperature of 1450°C for 2 h in H_2 gas. Microstructural observation revealed that the composite was composed entirely of Al_2O_3 and Fe-Co alloy. Neither residual metal oxides nor a reaction phase was observed. These results suggest that the ferrous alloy dispersed nanocomposite with sound microstructure and desired properties can be fabricated by controlled alloy system and powder processing.

Acknowledgement. This work was supported by grant No. 2000-1-30100-007-3 from the Basic Research Program of the Korea Science & Engineering Foundation.

This paper is dedicated to Professor Dr. Koichi Niihara on the occasion of his 60th birthday

References

1. K. Niihara, A. Nakahira and G. Sasaki: Proceed. of the First MRS Intern. Meeting on Advanced Mater., M. Doyama, S. Somiya and R.P.H. Chang (Ed.), Vol. 4, Pittsburg, PA (1989) 129.
2. K. Niihara: J. Ceram. Soc. Jpn., **99** (1991) 974.
3. Y. K. Jeong and K. Niihara: Nanostruct. Mater., **9** (1997) 193.
4. T. Sekino, T. Nakajima, S. Ueda and K. Niihara: J. Am. Ceram. Soc., **80** (1997) 1139.
5. S.-T. Oh, M. Sando and K. Niihara: J. Am. Ceram. Soc.,

81 (1998) 3013.
6. J. S. Lee, T. H. Kim, J. H. Yu and S. W. Chung: Nanostr. Mater., **9** (1997) 153.
7. D. R. Gaskell: Introduction to the Thermodynamics of Materials, Taylor & Francis, London (1995) 370.
8. J. G. Nam and J. S. Lee: Nanostr. Mater., **12** (1999) 475.
9. H. Mori and H. Yasuda: J. Microscopy, **180** (1995) 33.
10. B. Budiansky, J. C. Amazigo and A. G. Evans: J. Mech. Phys. Solids, **36** (1988) 167.
11. B. D. Cullity: Introduction to Magnetic Materials, Addison-Wesley Publ. Co., Massachusetts (1972) 525.
12. X. Y. Qin, J. G. Kim and J. S. Lee: Nanostr. Mater., **11** (1999) 259.